

# Joint mineral physics and seismic wave traveltime analysis of upper mantle temperature

Jeroen Ritsema<sup>1</sup>, Paul Cupillard<sup>2</sup>, Benoit Tauzin<sup>3</sup>, Wenbo Xu<sup>1</sup>, Lars Stixrude<sup>4</sup>, Carolina Lithgow-Bertelloni<sup>4</sup>

<sup>1</sup>Department of Geological Sciences, University of Michigan, Ann Arbor, Michigan 48109, USA

<sup>2</sup>Seismological Laboratory, University of California–Berkeley, Berkeley, California 94720, USA

<sup>3</sup>Ecole et Observatoire des Sciences de la Terre, Institut de Physique du Globe de Strasbourg, 67084 Strasbourg, France

<sup>4</sup>Department of Earth Sciences, University College London, London WC1E 6BT, UK

## ABSTRACT

We employ a new thermodynamic method for self-consistent computation of compositional and thermal effects on phase transition depths, density, and seismic velocities. Using these profiles, we compare theoretical and observed differential traveltimes between P410s and P( $T_{410}$ ) and between P660s and P410s ( $T_{660-410}$ ) that are affected only by seismic structure in the upper mantle. The anticorrelation between  $T_{410}$  and  $T_{660-410}$  suggests that variations in  $T_{410}$  and  $T_{660-410}$  of ~8 s are due to lateral temperature variations in the upper mantle transition zone of ~400 K. If the mantle is a mechanical mixture of basaltic and harzburgitic components, our traveltime data suggest that the mantle has an average temperature of  $1600 \pm 50$  K, in agreement with temperature estimates from magma compositions of mid-ocean ridge basalts. We infer a 100 K hotter mantle if we assume the mantle to have a homogeneous pyrolytic composition. The transition-zone temperature beneath hotspots and within subduction zones is relatively high and low, respectively. However, the largest variability in  $T_{410}$  and  $T_{660-410}$  is recorded by global stations far from subduction zones and hotspots. This indicates that the 400 K variation in upper mantle temperature is complicated by tilted upwellings, slab flattening and accumulation, ancient subduction, and processes unrelated to present-day subduction and plume ascent.

## INTRODUCTION

Constraints on the variation of temperature in the Earth's mantle are critical for our understanding of Earth's convective behavior. The best constraints on temperature in the deeper parts of the mantle are obtained from seismic studies. In particular, analyses of traveltimes of reflected (Shearer, 1991) and converted (Vinnik, 1977) waves that have interacted with wave speed and density discontinuities due to the olivine to wadsleyite (the 410 km) and the ringwoodite to perovskite + ferropericlasite (the 660 km) phase transitions, yield localized constraints on temperature in the transition zone (the region between the 410 km and the 660 km transitions). Since their Clapeyron slopes have opposite signs (Katsura and Ito, 1989), the 410 km transition is raised in a relatively cold upper mantle while the 660 km transition is lowered, thereby thickening the transition zone. Opposite deflections of the 410 km and 660 km and, hence, thinner transition zones, characterize the relatively warm regions of the upper mantle (Bina and Helffrich, 1994).

We introduce a new thermometer for the upper mantle based on a combination of mineral physics constraints and the analysis of traveltimes of compressional waves that have converted to shear waves in the transition zone. Contrary to previous global studies (Chevrot et al., 1999; Lawrence and Shearer, 2006; Tauzin et al., 2008), we do not infer the temperature from estimates of transition zone thickness that rely on upper mantle velocity corrections. Instead, our analysis employs theoretical one-dimensional profiles of seismic velocity based on realistic upper mantle bulk compositions and geotherms. These profiles account for the full complexity of the phase diagram and include all the mineralogical and thermal effects on phase transition depths, density, and wave speeds. Hence, they enable us to constrain the potential temperature of the mantle from traveltimes directly and self-consistently.

## CONVERTED WAVE TRAVELTIMES

Teleseismic P wave conversions, denoted as Pds, propagate as compressional (P) waves through the deep mantle and convert to shear (S) waves at an upper mantle discontinuity at depth  $d$  beneath the seismometer. The phases P410s and P660s, for example, are waves that have converted from P to S at the 410 km and the 660 km transitions, respectively (Fig. 1).

Our data are recorded traveltime differences between the phases P410s and P( $T_{410}$ ) and between P660s and P410s ( $T_{660-410}$ ).  $T_{410}$  and  $T_{660-410}$  are unaffected by imprecise earthquake locations and lower mantle heterogeneity. Although P410s and P660s are weak signals, they have predictable slowness (i.e., angle of incidence at the surface). It is therefore straightforward to enhance P410s and P660s amplitudes by summation (stacking) of a large (>50–100) number of teleseismic (epicentral distances >4000 km) receiver functions from regional (Li et al., 2000; Shen et al., 1998; Simmons and Gurrola, 2000) or global (Chevrot et al., 1999; Lawrence and Shearer, 2006; Tauzin et al., 2008) networks.

We consider two sets of  $T_{410}$  and  $T_{660-410}$  measurements. The first set is derived from ~7000 shallow (depth <50 km) earthquake recordings at broadband seismic instruments in California. These recordings feature simple first-arriving P waves that have amplitudes at least three times larger than the coda. We measure the variation in  $T_{410}$  and  $T_{660-410}$  using multiple stacks with common P410s conversion points within circular caps with radii of 1.5° across California and portions of adjacent states (Fig. 2). The second set of  $T_{410}$  and  $T_{660-410}$  measurements is from the study of Tauzin et al. (2008).  $T_{410}$  and  $T_{660-410}$  from this data set are measured using single-station stacks for 167 global network stations. It is the most

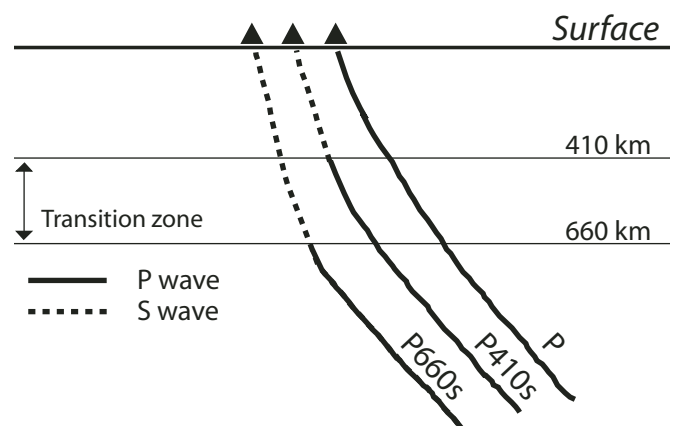


**Figure 1.** Ray paths of teleseismic P, P410s, and P660s through upper mantle. Phase P410s converts from P to S wave at 410 km discontinuity, while P660s converts from P to S at 660 km discontinuity. P wave and S wave segments are indicated by solid and dashed lines, respectively. Note that P, P410s, and P660s have nearly parallel P wave propagation paths in the lower mantle and that P410s and P660s differ only in the transition zone. Differential traveltimes  $T_{410}$  and  $T_{660-410}$  are affected only by structure in upper 660 km of mantle.

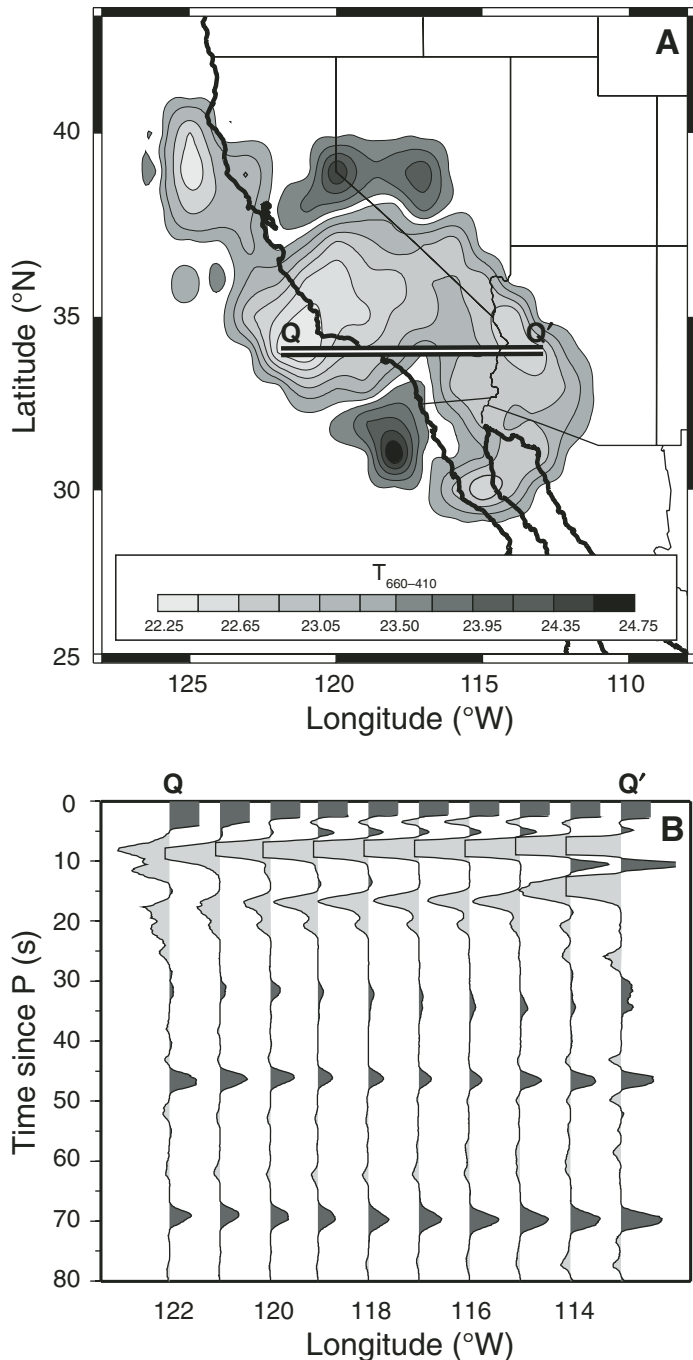


**Figure 2. A:** Map of  $T_{660-410}$  across California. **B:** West-east-oriented section (Q–Q') of receiver function stacks with common P410s conversion points along 34°N parallel with longitudes ranging from 122°W to 113°W. Q–Q' is indicated in A by horizontal line.

extensive global set of  $T_{410}$  and  $T_{660-410}$  collected to date, offering a global perspective (Fig. 3) with stations in subduction zones, near hotspots, and in diverse continental terrains.

Within California, average values for  $T_{410}$  and  $T_{660-410}$  are 45.5 s and 22.8 s, respectively. These values are  $\sim 2.1$  s larger and 0.7 s smaller than ak135 (Kennett et al., 1995) predicted values, respectively. They are in agreement with a previous estimate for station PAS in southern California (Gurrola and Minster, 1998) and stations in the western United States (Gilbert et al., 2003), and similar to most of the hotspot measurements from the global data set. The large value for  $T_{410}$  (compared to the ak135

predicted value) in California is due to reduced shear velocities in the relatively warm uppermost mantle beneath western North America.

The set of global  $T_{410}$  measurements exhibits a broad variation due to the relatively strong (thermal and compositional) heterogeneity in the uppermost 200–300 km of mantle.  $T_{410}$  peaks near 43.5 s, a value that is nearly identical to the ak135 predicted value.  $T_{410}$  measurements are skewed to low values because the majority of global seismic stations are located on relatively cool continental lithosphere. The global set of  $T_{660-410}$  has a narrower distribution than  $T_{410}$ .  $T_{660-410}$  is sensitive only to transition zone thickness and velocity variations.

## TRAVELTIME PREDICTIONS

We determine theoretical values of  $T_{410}$  and  $T_{660-410}$  from the velocity profiles of Xu et al. (2008), computed using the self-consistent thermodynamic method of Stixrude and Lithgow-Bertelloni (2005a, 2005b) and the updated parameters in Xu et al. (2008). For a given mantle composition and geotherm, velocity profiles are determined by computing equilibrium phase assemblages, the physical properties of the individual phases via stress and temperature derivatives of the Gibbs free energy, and the elastic properties of the assemblage from the Voigt-Reuss-Hill average.  $T_{410}$  and  $T_{660-410}$  are determined using reflectivity seismograms (Fuchs and Muller, 1971) that fully incorporate the effects on P410s and P660s waveforms due to the abrupt 410 km and 660 km and the gradual transformations in the non-olivine components.

Xu et al. (2008) considered the mantle to be a mixture of basalt ( $X_b$ ) and harzburgite ( $X_h$ ) with a basalt fraction of 18%. They considered two models of identical bulk composition that represent contrasting views of the reequilibration of subducted heterogeneity: (1) The equilibrium assemblage (EA) represents perfect re-equilibration of basalt and harzburgite into a homogeneous pyrolite. (2) The mechanical mixture (MM) maintains perfect disequilibrium. The MM value is motivated by the suggestion that the compositionally stratified oceanic lithosphere is responsible for heterogeneity in the mantle (Allègre and Turcotte, 1986).

## RESULTS

Figure 4 compares  $T_{410}$  and  $T_{660-410}$  for both the California and global data sets to theoretical values for the MM and EA and a range of adiabatic geotherms with potential temperature that vary between 1400 K and 1800 K. Low values for  $T_{410}$  and high values for  $T_{660-410}$  are recorded at stations in subduction zones. High and low values for  $T_{410}$  and  $T_{660-410}$  are recorded at hotspot stations above putative mantle plumes, as expected if the traveltime variations reflect temperature heterogeneity in the mantle. However, the total global variation in  $T_{410}$  and  $T_{660-410}$  among the normal stations is as large as the differences in  $T_{410}$  and  $T_{660-410}$  between hotspot and subduction zone stations.

Our computations indicate that the range in  $T_{410}$  and  $T_{660-410}$  values of  $\sim 8$  s can be explained by MM for geotherms with potential temperatures between 1400 K and 1800 K. The EA predicts 1–1.5 s higher values for  $T_{660-410}$  than the MM along the same adiabat since shear velocities in EA are lower (Xu et al., 2008). Consequently, the potential temperature that provides the best match to  $T_{410}$  and  $T_{660-410}$  is  $\sim 100$  K higher for the EA.  $T_{410}$  and  $T_{660-410}$  within California and all hotspot stations can be matched by MM structure with a potential mantle temperature of 1650–1700 K.

## DISCUSSION AND CONCLUSIONS

The systematic mismatch between observed and predicted values for  $T_{410}$  stems from simplifications in our calculations. First, we assume adiabatic geotherms, ignoring the thermal boundary layer of the lithosphere. Second, we invoke a homogeneous pyrolitic composition for the mantle, but most seismic stations are located on continental lithosphere with a depleted composition. In addition,  $T_{410}$  and  $T_{660-410}$  may be influenced by the presence of water (Litasov et al., 2005). Variations in bulk composition

**Figure 3.** Left: Measurements of  $T_{410}$  and  $T_{660-410}$  (Tauzin et al., 2008) plotted at global station locations. Values of  $T_{410}$  and  $T_{660-410}$  larger and smaller than predicted values for MM 1600 (mechanical mixture composition and geotherm with  $T_p$  of 1600 K) are indicated by triangles and circles, respectively. Right: Histograms of  $T_{410}$  and  $T_{660-410}$ . Predicted values for  $T_{410}$  and  $T_{660-410}$  by MM 1600 are indicated by dashed lines.

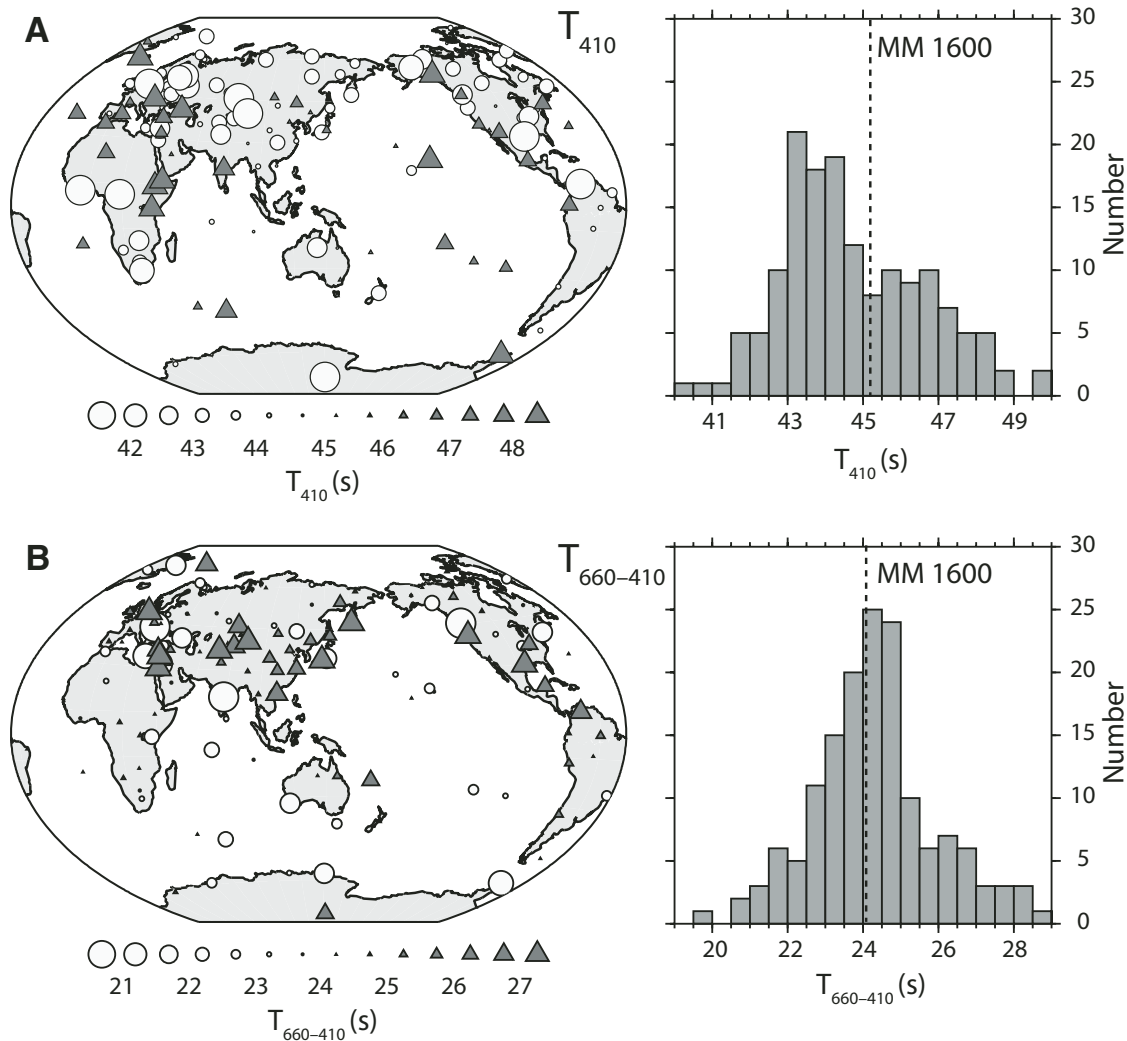
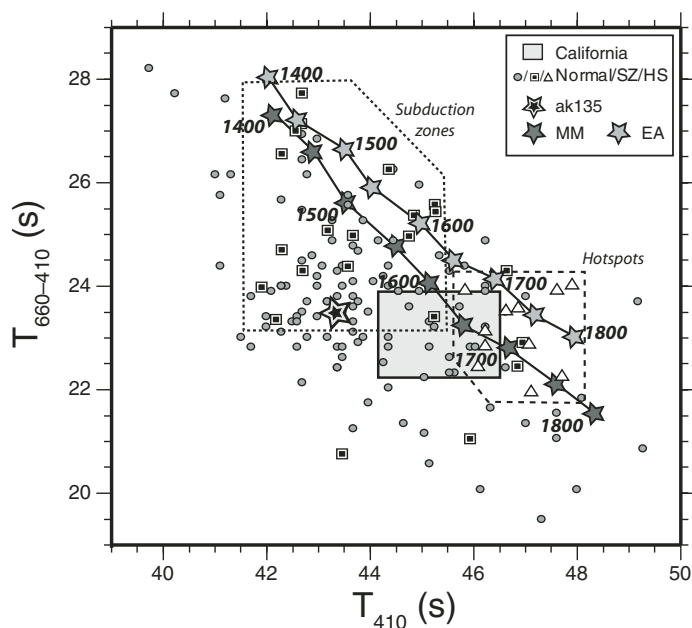


**Figure 4.** Measurements of  $T_{660-410}$  and  $T_{410}$  at global (circles, squares, and triangles) and regional (gray rectangle) network stations in California. Dashed lines encompass hotspot (HS) (triangles) data. Dotted lines encompass data from all but three subduction zones, (SZ) (squares). Theoretical traveltimes are computed for ak135 (black star; after Kennett et al., 1995), EA (equilibrium assemblage; light gray stars), and MM (mechanical mixture; dark gray stars) compositions for adiabatic geotherms with potential temperatures ranging from 1400 K to 1800 K.



within the upper mantle (Cobden et al., 2008) may also influence  $T_{410}$  and  $T_{660-410}$ . In fact, the MM model renders a natural way to develop radial gradients in composition (Christensen and Hofmann, 1994; Xie and Tackley, 2004), although we have found (Ritsema et al., 2008; Xu et al., 2008) that changes in basalt fraction in a mechanically mixed mantle have little effect on wave speeds in the transition zone.

Nevertheless, the trends in  $T_{410}$  and  $T_{660-410}$  suggest strongly that temperature variations in the mantle are largely responsible for the observed traveltime variation. The seismic data can be reconciled with upper mantle geotherms whose potential temperatures vary between 1400 K

and 1800 K, if we assume that the mantle is composed of a mechanical mixture of basalt and harzburgite with a pyrolitic bulk composition. An average mantle temperature of  $1600 \pm 50$  K and perturbations of as much as 200 K agree well with temperature estimates from magma compositions of mid-ocean ridge basalts (Herzberg et al., 2007; Putirka, 2008). For the EA model, which features a homogeneous pyrolite composition, inferred temperatures are 100 K higher than for the MM and appear inconsistent with geochemical estimates. Thus our calculations indicate that the MM composition and the 1600 K geotherm provide a useful reference for studying the structure and dynamics of Earth's interior.

The temperature difference between subduction zones and hotspot regions is  $\sim 400$  K. It likely underestimates the true contrast, given that we sample wide ( $>500$  km) regions of the mantle due to data stacking and averaging. The predominantly low values of  $T_{660-410}$  and high values of  $T_{410}$  at hotspot stations indicate elevated temperatures throughout the upper mantle beneath hotspots, in agreement with Lawrence and Shearer (2006) and Courtier et al. (2007). However, hotspots and putative plumes are not the sole hot regions of Earth's mantle. The temperature in the mantle is equally high beneath California and adjacent western states, a region characterized by anomalous tectonic processes but not deep mantle upwelling. Mantle upwellings may be tilted (Benoit et al., 2006; Ritsema et al., 1999), and relatively warm regions may not cause hotspot volcanism. Moreover, the transition zone may be cooled by the ponding and flattening of slabs (Fukao et al., 2001; Gu et al., 2001) and by the continental lithosphere (Sine et al., 2008), indicating that the thermal state of the mantle is governed by ancient as well as recent processes.

#### ACKNOWLEDGMENTS

Data have been provided by the Incorporated Research Institutions for Seismology/Data Management System (IRIS/DMC), the Northern California Earthquake Data Center, and the Southern California Earthquake Data Center. Figures in the paper have been produced using the Generic Mapping Tools software of Wessel and Smith (1995). We thank Saskia Goes and Keith Putirka for constructive reviews. The research has been supported by National Science Foundation grant EAR-0609763.

#### REFERENCES CITED

- Allègre, C.J., and Turcotte, D.L., 1986, Implications of the two-component marble-cake mantle: *Nature*, v. 323, p. 123–127, doi: 10.1038/323123a0.
- Benoit, M.H., Nyblade, A.A., and VanDecar, J.C., 2006, Upper mantle P wave speed variations beneath Ethiopia and the origin of the Afar hotspot: *Geology*, v. 34, p. 329–332.
- Bina, C.R., and Helffrich, G., 1994, Phase transition Clapeyron slopes and transition zone seismic discontinuity topography: *Journal of Geophysical Research*, v. 99, p. 15,853–15,860, doi: 10.1029/94JB00462.
- Chevrot, S., Vinnik, L., and Montagner, J.-P., 1999, Global-scale analysis of the mantle Pds phases: *Journal of Geophysical Research*, v. 104, p. 20,203–20,219, doi: 10.1029/1999JB900087.
- Christensen, U.R., and Hofmann, A.W., 1994, Segregation of subducted oceanic crust and the convecting mantle: *Journal of Geophysical Research*, v. 99, p. 19,867–19,884, doi: 10.1029/93JB03403.
- Cobden, L., Goes, S., Cammarano, F., and Connolly, J.A.D., 2008, Thermochemical interpretation of one-dimensional seismic reference models for the upper mantle: Evidence for bias due to heterogeneity: *Geophysical Journal International*, v. 175, p. 627–648, doi: 10.1111/j.1365-246X.2008.03903.x.
- Courtier, A.M., and 14 others, 2007, Correlation of seismic and petrologic thermometers suggests deep thermal anomalies beneath hotspots: *Earth and Planetary Science Letters*, v. 264, p. 308–316, doi: 10.1016/j.epsl.2007.10.003.
- Fuchs, K., and Muller, G., 1971, Computation of synthetic seismograms with the reflectivity method and comparison with observations: *Royal Astronomical Society Geophysical Journal*, v. 23, p. 417–433.
- Fukao, Y., Widiyantoro, S., and Obayashi, M., 2001, Stagnant slabs in the upper and lower mantle transition region: *Reviews of Geophysics*, v. 39, p. 291–324, doi: 10.1029/1999RG000068.
- Gilbert, H.J., Sheehan, A.F., Dueker, K.G., and Molnar, P., 2003, Receiver functions in the western United States, with implications for upper mantle structure and dynamics: *Journal of Geophysical Research*, v. 108, no. B5, 2229, doi: 10.1029/2001JB001194.
- Gu, Y.J., Dziewonski, A.M., Su, W., and Ekstrom, G., 2001, Models of the mantle shear velocity and discontinuities in the pattern of lateral hetero-

- geneities: *Journal of Geophysical Research*, v. 106, p. 11,169–11,199, doi: 10.1029/2001JB000340.
- Gurrola, H., and Minster, B., 1998, Thickness estimates of the upper-mantle transition zone from bootstrapped velocity spectrum stacks of receiver functions: *Geophysical Journal International*, v. 133, p. 31–43, doi: 10.1046/j.1365-246X.1998.1331470.x.
- Herzberg, C., Asimow, P.D., Arndt, N., Niu, Y., Leshner, C.M., Fitton, J.G., Cheadle, M.J., and Saunders, A.D., 2007, Temperatures in ambient mantle and plumes: Constraints from basalts, picrites, and komatiites [abs.]: *Geochemistry, Geophysics, Geosystems*, v. 8, Q02006, doi: 10.1029/2006GC001390.
- Katsura, T., and Ito, E., 1989, The system Mg (sub 2) SiO (sub 4) -Fe (sub 2) SiO (sub 4) at high pressures and temperatures; precise determination of stabilities of olivine, modified spinel, and spinel: *Journal of Geophysical Research*, v. 94, p. 15,663–15,670, doi: 10.1029/JB094iB11p15663.
- Kennett, B.L.N., Engdahl, E.R., and Buland, R., 1995, Constraints on seismic velocities in the Earth from traveltimes: *Geophysical Journal International*, v. 122, p. 108–124, doi: 10.1111/j.1365-246X.1995.tb03540.x.
- Lawrence, J.F., and Shearer, P.M., 2006, A global study of transition zone thickness using receiver functions: *Journal of Geophysical Research*, v. 111, B06307, doi: 10.1029/2005JB003973.
- Li, X., Sobolev, S.V., Kind, R., Yuan, X., and Estabrook, C., 2000, A detailed receiver function image of the upper mantle discontinuities in the Japan subduction zone: *Earth and Planetary Science Letters*, v. 183, p. 527–541, doi: 10.1016/S0012-821X(00)00294-6.
- Litasov, K.D., Ohtani, E., Sano, A., Suzuki, A., and Funakoshi, K., 2005, Wet subduction versus cold subduction: *Geophysical Research Letters*, v. 32, L13312, doi: 10.1029/2005GL022921.
- Putirka, K., 2008, Excess temperatures at ocean islands: Implications for mantle layering and convection: *Geology*, v. 36, p. 283–286, doi: 10.1130/G24615A.1.
- Ritsema, J., van Heijst, H.J., and Woodhouse, J.H., 1999, Complex shear wave velocity structure imaged beneath Africa and Iceland: *Science*, v. 286, p. 1925–1928, doi: 10.1126/science.286.5446.1925.
- Ritsema, J., Xu, W., Stixrude, L., and Lithgow-Bertelloni, C., 2009, Estimates of the transition zone temperature in a mechanically mixed upper mantle: *Earth and Planetary Science Letters*, v. 277, p. 244–252, doi: 10.1016/j.epsl.2008.10.024.
- Shearer, P.M., 1991, Constraints on upper mantle discontinuities from observations of long-period reflected and converted phases: *Journal of Geophysical Research*, v. 96, p. 18,147–18,182, doi: 10.1029/91JB01592.
- Shen, Y., Solomon, S.C., Bjarnason, I.T., and Wolfe, C., 1998, Seismic evidence for a lower mantle origin of the Iceland plume: *Nature*, v. 395, p. 62–65, doi: 10.1038/25714.
- Simmons, N.A., and Gurrola, H., 2000, Multiple seismic discontinuities near the base of the transition zone in the Earth's mantle: *Nature*, v. 405, p. 559–562, doi: 10.1038/35014589.
- Sine, C.R., Wilson, D., Gao, W., Grand, S.P., Aster, R., Ni, J., and Baldrige, W.S., 2008, Mantle structure beneath the western edge of the Colorado Plateau: *Geophysical Research Letters*, v. 35, L10303, doi: 10.1029/2008GL033391.
- Stixrude, L., and Lithgow-Bertelloni, C., 2005a, Mineralogy and elasticity of the oceanic upper mantle: Origin of the low-velocity zone: *Journal of Geophysical Research*, v. 110, B03204, doi: 10.1029/2004JB002965.
- Stixrude, L., and Lithgow-Bertelloni, C., 2005b, Thermodynamics of mantle minerals—I. Physical properties: *Geophysical Journal International*, v. 162, p. 610–632, doi: 10.1111/j.1365-246X.2005.02642.x.
- Tauzin, B., Debayle, E., and Wittlinger, G., 2008, The mantle transition zone as seen by global Pds phases: No clear evidence for a thin transition zone beneath hotspots: *Journal of Geophysical Research*, v. 113, B08309, doi: 10.1029/2007JB005364.
- Vinnik, L.P., 1977, Detection of waves converted from P to SV in the mantle: *Physics of the Earth and Planetary Interiors*, v. 15, p. 39–45, doi: 10.1016/0031-9201(77)90008-5.
- Wessel, P., and Smith, W.H.F., 1995, New version of the Generic Mapping Tools released: *Eos (Transactions, American Geophysical Union)*, v. 76, p. 329, doi: 10.1029/95EO00198.
- Xie, S., and Tackley, P.J., 2004, Evolution of helium and argon isotopes in a convecting mantle: *Earth and Planetary Science Letters*, v. 146, p. 417–439.
- Xu, W., Lithgow-Bertelloni, C., Stixrude, L., and Ritsema, J., 2008, The effect of bulk composition and temperature on mantle seismic structure: *Earth and Planetary Science Letters*, v. 275, p. 70–79, doi: 10.1016/j.epsl.2008.08.012.

Manuscript received 19 August 2008

Revised manuscript received 19 November 2008

Manuscript accepted 1 December 2008

Printed in USA